12-12-2007

Effects of Dielectric Relaxation on the Director Dynamics of Uniaxial Nematic Liquid Crystals

Mingxia Gu
Kent State University - Kent Campus, gu@lci.kent.edu

Ye Yin
Kent State University - Kent Campus

Sergij V. Shiyanovskii
Kent State University - Kent Campus

Oleg Lavrentovich
Kent State University - Kent Campus, olavrent@kent.edu

Effects of dielectric relaxation on the director dynamics of uniaxial nematic liquid crystals

Mingxia Gu, Ye Yin, Sergij V. Shiyanovskii, and Oleg D. Lavrentovich
Chemical Physics Interdisciplinary Program, Liquid Crystal Institute, Kent State University, Kent, Ohio 44242, USA
(Received 20 September 2007; published 12 December 2007)

The dielectric anisotropy of liquid crystals causes director reorientation in an applied electric field and is thus at the heart of electro-optic applications of these materials. The components of the dielectric tensor are frequency dependent. Until recently, this frequency dependence was not accounted for in a description of director dynamics in an electric field. We theoretically derive the reorienting dielectric torque acting on the director, taking into account the entire frequency spectrum of the dielectric tensor. The model allows one to include the effects of multiple relaxations in both parallel and perpendicular components of the dielectric tensor, thus generalizing a recent model [Y. Yin *et al.*, Phys. Rev. Lett. **95**, 087801 (2005)] limited by the single-relaxation approach. The model predicts the "dielectric memory effect" (DME)—i.e., dependence of the dielectric torque on both the "present" and "past" values of the electric field and the director. The model describes the experimentally observed director reorientation in the case when the rise time of the applied voltage is smaller than the dielectric relaxation time. In typical materials such as pentylcyanobiphenyl (5CB), in which the dielectric anisotropy is positive at low frequencies, the DME slows down the director reorientation in a sharply rising electric field, as the sharp front is perceived as a high-frequency excitation for which the dielectric anisotropy is small or even of a negative sign. In materials that are dielectrically negative, the DME speeds up the response when a sharp pulse is applied.

DOI: 10.1103/PhysRevE.76.061702 PACS number(s): 61.30.Dk, 42.79.Kr, 77.22.Gm, 77.84.Nh

I. INTRODUCTION

The anisotropy of the dielectric permittivity of liquid crystals (LCs) is one of the most important features of these materials. It leads to the phenomenon of director reorientation in the electric field. The latter, often called the Frederiks effect, has numerous electro-optical applications, most notably in LC displays [1–3]. Until very recently, a theoretical description of the effect has been limited by the assumption that the dielectric response is instantaneous. Namely, it was assumed that the electric displacement $\mathbf{D}$ at the moment of time t is determined solely by the electric field $\mathbf{E}$ acting on the LC at the very same moment t. In other words, the effects of a finite rate of dielectric relaxation have been neglected. Such an approach is certainly valid when the characteristic rise time τ_U of the voltage driving the LC cell is much longer than the time of the dielectric relaxation, τ_r. However, modern applications require faster and faster switching speed and a number of researchers have demonstrated fast switching by decreasing the rise time of the driving voltage, down to values comparable to the characteristic dielectric relaxation time, $\tau_U \leqslant \tau_r$, which is in the range of tens of nanoseconds for materials such as the classic 4−*n*-pentyl-4′-cyanobiphenyl (5CB) [4], and in the microsecond range for the so-called dual-frequency nematics (DFNs) [5]. In the DFNs, the dielectric anisotropy $\Delta\varepsilon = \varepsilon_\parallel - \varepsilon_\perp$ is positive at low frequencies f and negative at high f; the frequency at which $\Delta\varepsilon$ changes sign is called the crossover frequency f_c. Here, $\varepsilon_\parallel$ and $\varepsilon_\perp$ are the components of dielectric permittivity tensor measured parallel to the director $\hat{\mathbf{n}}$ and perpendicular to it, respectively. In the regime $\tau_U \leqslant \tau_r$, the assumption of an instantaneous response is not valid anymore and experimental observations can no longer be explained by the conventional theory of dielectric response [6]. For example, a sharp increase of the applied dc voltage is perceived by the LC as a high-frequency ac excitation that in DFNs might lead a curious behavior of $\hat{\mathbf{n}}$ that first reorients away from the direction of $\mathbf{E}$ and then realigns parallel to it, as has been demonstrated both experimentally [6] and theoretically [6,7].

To describe the "dielectric memory effect" (DME)—i.e., dielectrically induced $\hat{\mathbf{n}}$ reorientation in the regime $\tau_U \leqslant \tau_r$—we previously developed a model [6] of dielectric response in which the dielectric torque density has been calculated for a nematic LC in which $\varepsilon_\parallel$ experiences just one relaxation with a characteristic time τ_r; $\varepsilon_\perp$ was assumed to be a frequency-independent constant. For $\tau_U \gg \tau_r$, the model [6] coincides with the classic theory, in which the director dynamics depends only on the "instantaneous" $\mathbf{E}$ and the effective $\Delta\varepsilon$ that measures the strength and direction of the dielectric torque is determined by its value at low f. For $\tau_U \leqslant \tau_r$, however, the model [6] predicts a very different scenario: the dielectric torque contains, in addition to the standard "instantaneous" contribution, which in this case has an effective $\Delta\varepsilon$ that corresponds to the high f, also a "memory" contribution proportional to the difference in $\varepsilon_\parallel$ values at low and high f's. Not only do the "instantaneous" and "memory" terms depend on different values of permittivities; they are even of opposite signs in DFNs, enabling the curious effect mentioned above: namely, reorientation of $\hat{\mathbf{n}}$ away from $\mathbf{E}$ and then parallel to $\mathbf{E}$ when the DFN is driven by a sharp voltage pulse. A similar model that also considered a single Debye-type relaxation process in the parallel permittivity of a DFN has been proposed by Mottram and Brown [7].

The single-relaxation assumption of the models [6,7] is certainly a limitation, as most LCs exhibit multiple processes of relaxation that involve not only $\varepsilon_\parallel$ but also $\varepsilon_\perp$ [8]. In this article, we generalize the description of the DME [6] by lifting the restriction of a single-relaxation process and considering multiple relaxations that might occur in both $\varepsilon_\parallel$ and $\varepsilon_\perp$. The generalized model allows us to extend the description from a relatively limited class of proper DFNs with τ_r

$\sim 0.01-1$ ms, to practically the entire class of nematic LCs which include materials such as cyanobiphenyls, typical compounds used in electro-optical research and applications, with τ_r in the range of nanoseconds. Note that many "regular" LCs with positive dielectric anisotropy, such as cyanobiphenyls, are in fact also DFNs, with the difference that f_c is in the MHz region [9–12] rather than in the kHz range. The model also allows us to describe materials with multiple relaxations, as we demonstrate in the example of mixtures of 5CB and MLC2048. Finally, it allows one to optimize the driving schemes of LC cells to achieve a faster response time.

Below, we start with the theoretical model and then describe the experimental data relevant to different scenarios of dielectric relaxation. Namely, we study 5CB as an example of a material with relaxations in both $\varepsilon_\parallel$ and $\varepsilon_\perp$, mixtures of 5CB with MLC2048 in which there are multiple relaxations of $\varepsilon_\parallel$, and finally, a material with $\Delta\varepsilon<0$ in which the DME leads to a faster response time (as opposed to the case of $\Delta\varepsilon>0$ in which the DME delays the director reorientation).

II. THEORY

The LC director reorients in an applied electric field under the action of the dielectric torque, whose density is [3] $\mathbf{M}(t)=\mathbf{D}(t)\times\mathbf{E}(t)$, where $\mathbf{E}(t)$ and $\mathbf{D}(t)$ are the electric field and electric displacement at the moment of time t, respectively. In the widely accepted standard approach, $\mathbf{D}(t)$ is determined by the instantaneous current electric field—i.e., $\mathbf{D}(t)=\varepsilon_0\boldsymbol{\varepsilon}\mathbf{E}(t)$, where ε_0 is the vacuum dielectric constant and $\boldsymbol{\varepsilon}$ is the relative dielectric permittivity tensor. However, when $\tau_U \leqslant \tau_r$, the dielectric relaxation will affect the director reorientation and can no longer be ignored [6,7]. Below, we develop a model of dielectric response in the uniaxial nematic LCs by taking into account that both $\varepsilon_\parallel$ and $\varepsilon_\perp$ might experience multiple relaxations with an increase of f.

Using the superposition rule [13], $\mathbf{D}(t)$ can be written as

$$\mathbf{D}(t)=\varepsilon_0\mathbf{E}(t)+\int_{-\infty}^{t}\mathbf{P}(t,t')dt'$$

$$=\varepsilon_0\mathbf{E}(t)+\varepsilon_0\int_{-\infty}^{t}\boldsymbol{\alpha}(t,t')\mathbf{E}(t')dt', \tag{1}$$

where $\mathbf{P}(t,t')$ represents the polarization component, which describes the contribution of the past electric field $\mathbf{E}(t')$ to the current polarization. The step response function $\boldsymbol{\alpha}(t,t')$ is also called the decay function, since it vanishes when $t-t'\to\infty$. When the dielectric properties of the medium do not change with time, for example, in solid crystals, $\boldsymbol{\alpha}(t,t')$ can be described as a function of time interval $t-t'$; i.e.,

$$\boldsymbol{\alpha}(t,t')=\boldsymbol{\alpha}(t-t'). \tag{2}$$

Equation (2) ensures that a harmonic field $\mathbf{E}(t)=\mathbf{E}_\omega e^{-i\omega t}$ leads to a harmonic electric displacement $\mathbf{D}(t)$ with the same angular frequency ω,

$$\mathbf{D}(t)=\varepsilon_0\left(\mathbf{I}+\int_0^\infty\boldsymbol{\alpha}(t-t')e^{i\omega(t-t')}d(t-t')\right)\mathbf{E}_\omega e^{-i\omega t}=\mathbf{D}_\omega e^{-i\omega t}. \tag{3}$$

Note that we use two notations for frequency: the cyclic frequency f and the angular frequency ω related in the standard way, $f=\omega/2\pi$. We define the frequency-dependent dielectric permittivity $\boldsymbol{\varepsilon}(\omega)$,

$$\boldsymbol{\varepsilon}(\omega)=\mathbf{I}+\int_0^\infty\boldsymbol{\alpha}(t-t')e^{i\omega(t-t')}d(t-t'), \tag{4}$$

where $\mathbf{I}$ is the unit tensor. Combining Eqs. (3) and (4), we obtain the dielectric response equation in the frequency domain:

$$\mathbf{D}(\omega)=\varepsilon_0\boldsymbol{\varepsilon}(\omega)\mathbf{E}_\omega. \tag{5}$$

Equation (2) and, therefore, Eq. (5) are not valid when the LC director reorients (it would be valid if $\hat{\mathbf{n}}$ is somehow frozen and does not reorient in the changing electric field). Below we search for the analog of Eq. (2) that takes into account the changes in the dielectric permittivity caused by director reorientation.

The dielectric response tensor function $\boldsymbol{\alpha}(t,t')$ of the nematic LCs is comprised of different relaxation modes $\boldsymbol{\alpha}_k(t,t')$:

$$\boldsymbol{\alpha}(t,t')=\sum_k\boldsymbol{\alpha}_k(t,t'). \tag{6}$$

If the kth relaxation process is sufficiently fast as compared to the change of electric field, the electric field and the director field can be considered as constant during the relaxation period; i.e.,

$$\int_{-\infty}^{t}\boldsymbol{\alpha}_k(t,t')\mathbf{E}(t')dt'=\mathbf{E}(t)\int_{-\infty}^{t}\bar{\boldsymbol{\alpha}}_k(t,t')dt', \tag{7}$$

where $\bar{\boldsymbol{\alpha}}_k(t,t')=\boldsymbol{\alpha}_k(t,t')$ for a fixed director orientation $\hat{\mathbf{n}}(t')=\hat{\mathbf{n}}(t)$. We split $\boldsymbol{\alpha}(t,t')$ into two terms: a "fast" one $\boldsymbol{\alpha}_f(t,t')$, which includes relaxations which are much faster than the director reorientation and the electric field change (and thus satisfy Eq. (7)), and a "slow" one $\boldsymbol{\alpha}_s(t,t')$:

$$\boldsymbol{\alpha}(t,t')=\boldsymbol{\alpha}_f(t,t')+\boldsymbol{\alpha}_s(t,t'). \tag{8}$$

Note that both fast and slow parts of $\boldsymbol{\alpha}(t,t')$ are sums of terms originating from different relaxation processes. Now we can rewrite the electric displacement $\mathbf{D}(t)$ in nematic LCs as

$$\mathbf{D}(t)=\varepsilon_0\boldsymbol{\varepsilon}_f(t)\mathbf{E}(t)+\varepsilon_0\int_{-\infty}^{t}\boldsymbol{\alpha}_s(t,t')\mathbf{E}(t')dt', \tag{9}$$

where the "fast" part $\boldsymbol{\varepsilon}_f$ of the relative dielectric permittivity tensor is defined as

$$\boldsymbol{\varepsilon}_f(t)=\mathbf{I}+\int_{-\infty}^{t}\boldsymbol{\alpha}_f(t,t')dt'. \tag{10}$$

In the local frame associated with the director, $\boldsymbol{\varepsilon}_f(t)$ has a stationary diagonal form; thus, its time dependence origi-

nates from reorientation of the local frame and is determined solely by the current director field $\hat{\mathbf{n}}(t)$:

$$\boldsymbol{\varepsilon}_f(t) = \varepsilon_{f\perp}\mathbf{I} + (\varepsilon_{f\parallel} - \varepsilon_{f\perp})\hat{\mathbf{n}}(t) \otimes \hat{\mathbf{n}}(t), \tag{11}$$

where $\varepsilon_{f\parallel}$ and $\varepsilon_{f\perp}$ are the components of the dielectric tensor in the diagonal form and $\otimes$ is the external product of two vectors, the operation result being a tensor with components $[\hat{\mathbf{n}}(t) \otimes \hat{\mathbf{n}}(t)]_{ij} = n_i(t)n_j(t)$.

When $\hat{\mathbf{n}}$ reorients, the polarization parallel to $\hat{\mathbf{n}}$ should be dragged by the director; this is because a high potential barrier arises when the polarization deviates from the long axes of molecules. This is also true for the rotation of the polarization perpendicular to $\hat{\mathbf{n}}$. It is also assumed that this dragging of polarization shall not affect the reorientation of individual molecules. This assumption is reasonable even when the rotation speed of $\hat{\mathbf{n}}$ is comparable to the relaxation speed of polarization, because the slow rotation of all molecules should not substantially affect the fast flip-flop of the small number of molecules which are responsible for the dielectric relaxation. In a local frame $\{\hat{\mathbf{l}}(t), \hat{\mathbf{m}}(t), \hat{\mathbf{n}}(t)\}$, where $\hat{\mathbf{l}}(t)$, $\hat{\mathbf{m}}(t)$, and $\hat{\mathbf{n}}(t)$ represent the three principal axes, rotating with an angular velocity $\Omega(t) = -\dot{\hat{\mathbf{n}}}(t) \times \hat{\mathbf{n}}(t)$, one can write

$$\dot{\hat{\mathbf{v}}}(t) = \boldsymbol{\Omega}(t) \times \hat{\mathbf{v}}(t) = -[\dot{\hat{\mathbf{n}}}(t) \times \hat{\mathbf{n}}(t)] \times \hat{\mathbf{v}}(t), \tag{12}$$

where $\hat{\mathbf{v}}(t) = \hat{\mathbf{l}}(t)$ or $\hat{\mathbf{m}}(t)$ or $\hat{\mathbf{n}}(t)$. The dielectric relaxation in this frame depends on $\hat{\mathbf{n}}$ rotation, and thus we can describe $\boldsymbol{\alpha}_s(t,t')$ in the laboratory frame by the diagonal components $\alpha_\parallel(t-t')$ along $\hat{\mathbf{n}}$ and $\alpha_\perp(t-t')$ perpendicular to $\hat{\mathbf{n}}$ when $\hat{\mathbf{n}}$ is fixed:

$$\boldsymbol{\alpha}_s(t,t') = \alpha_\parallel(t-t')\hat{\mathbf{n}}(t) \otimes \hat{\mathbf{n}}(t') + \alpha_\perp(t-t')\{\hat{\mathbf{l}}(t) \otimes \hat{\mathbf{l}}(t') + \hat{\mathbf{m}}(t) \otimes \hat{\mathbf{m}}(t')\}. \tag{13}$$

Therefore, we can write the dielectric torque density as

$$\mathbf{M}(t) = \mathbf{D}(t) \times \mathbf{E}(t) = \varepsilon_0 \left\{ (\varepsilon_{f\parallel} - \varepsilon_{f\perp})\hat{\mathbf{n}}(t)[\hat{\mathbf{n}}(t) \cdot \mathbf{E}(t)] + \int_{-\infty}^{t} \boldsymbol{\alpha}_s(t,t')\mathbf{E}(t')dt' \right\} \times \mathbf{E}(t). \tag{14}$$

The integral term in Eq. (14), absent in the conventional "instantaneous" dielectric response theory, describes the DME. The dielectric displacement $\mathbf{D}(t)$ depends on the prehistory of the electric field $\mathbf{E}(t')$.

Below, we demonstrate that the DME can also be described within an approach based on the free energy. We introduce the dielectric term $F_E(t)$ in the free-energy density of a LC cell under an applied voltage:

$$F_E(t) = -\left\{ \frac{1}{2}\{\varepsilon_0\varepsilon_{f\perp}\mathbf{E}^2(t) + (\varepsilon_{f\parallel} - \varepsilon_{f\perp})[\mathbf{n}(t) \cdot \mathbf{E}(t)]^2\} + \varepsilon_0\mathbf{E}(t)\int_{-\infty}^{t} \boldsymbol{\alpha}_s(t,t')\mathbf{E}(t')dt' \right\}, \tag{15}$$

where the electric field $\mathbf{E}(t) = -\boldsymbol{\nabla}V(t)$ satisfies Maxwell equation $\boldsymbol{\nabla} \times \mathbf{E}(t) = 0$. Variations of Eq. (15) allow one to find the distribution of the potential $V(t)$ inside the cell, $-\frac{\delta F_E(t)}{\delta V(t)} = \boldsymbol{\nabla} \cdot \mathbf{D}(t) = 0$, and to obtain Eq. (14):

$$\mathbf{M}(t) = \sum_{\hat{\mathbf{v}}(t)} \hat{\mathbf{v}}(t) \times \frac{\delta F_E(t)}{\delta \hat{\mathbf{v}}(t)}, \tag{16}$$

where $\hat{\mathbf{v}}(t) = \hat{\mathbf{l}}(t)$ or $\hat{\mathbf{m}}(t)$ or $\hat{\mathbf{n}}(t)$. Note that the numerical coefficients for the two terms in Eq. (15) are different, equal to "1/2" for the first ("instantaneous") term but to "1" for the second ("memory") term. The coefficient 1/2 enters the standard expression for the dielectric energy when change of the electric field is adiabatically slow and the system has enough time to respond. On the other hand, the coefficient value 1 corresponds to the energy of a permanent dipole in the electric field.

The slow step response functions $\alpha_\parallel(t-t')$ and $\alpha_\perp(t-t')$ in Eq. (13) can be reconstructed from the frequency dispersion of the dielectric tensor. Slow relaxation processes in LCs are caused by reorientation of permanent molecular dipoles and usually obey the classic Debye theory of dielectric relaxation [14], with an exponential decay behavior and a Lorenzian behavior in the frequency domain:

$$\alpha_\eta(t-t') = \sum_i^{p_\eta} \frac{\delta\varepsilon_{i\eta}}{\tau_{i\eta}} \exp\left(-\frac{t-t'}{\tau_{i\eta}}\right), \quad \eta = \parallel, \perp, \tag{17}$$

$$\alpha_\eta(\omega) = \sum_i^{p_\eta} \frac{\delta\varepsilon_{i\eta}}{1 - i\omega\tau_{i\eta}}, \quad \eta = \parallel, \perp, \tag{18}$$

where $\delta\varepsilon_{i\eta}$ and $\tau_{i\eta}$ are the dielectric "strength" and the relaxation time of the ith relaxation of parallel or perpendicular component, respectively; p_η is the number of slow relaxation processes for the parallel or perpendicular components of permittivity. Note that if the relaxation times of different processes are well separated, then the strength $\delta\varepsilon_{i\eta}$ of each of these processes can be defined in practice as the difference in the permittivities at frequencies below and above the characteristic frequency $\sim 1/\tau_{i\eta}$. If the relaxation times are close to each other, the value of $\delta\varepsilon_{i\eta}$ is found from the fitting of the dielectric permittivity dispersion curves. For other, non-Debye types of relaxations, such as Havriliak-Negami, Fuoss-Kirwood, or generalized Cole-Cole types [8], Eqs. (13)–(16) are still valid and one only needs to modify Eqs. (17) and (18).

To get a better insight into the physics of the DME and the ways it can be verified experimentally, we consider below a typical case of a homogeneously aligned nematic cell subject to an electric field $\mathbf{E}(t)$ along the z axis that is normal to the bounding plates, Fig. 1. Let $\theta(z,t)$ be the angle between $\hat{\mathbf{n}}(t)$ and the normal to the substrate at the time t, measured at a point z. We assume that $\theta(z,t)$ does not depend on the in-plane x,y coordinates and that the director rotates only in the x-z plane (x axis is the projection of the alignment axis onto the cell substrates). The Erickson-Leslie equation describing the director dynamics in absence of material flow then can be written as [15,16]

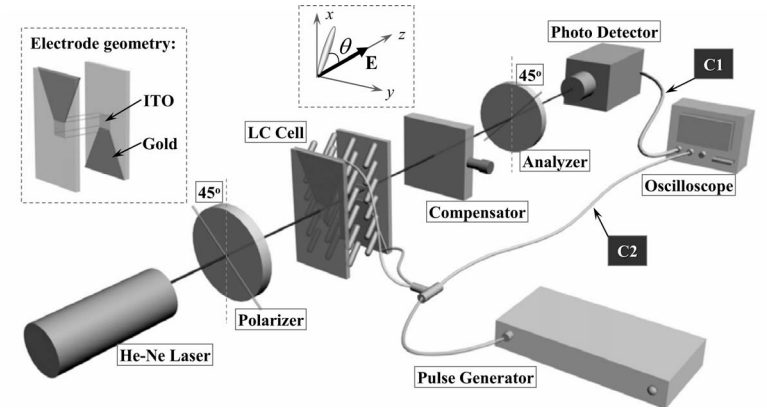

FIG. 1. Experimental setup for the DME experiment.

$$-\gamma_1 \frac{\partial \theta(z,t)}{\partial t} = M(t) - [K_1 \sin^2 \theta(z,t) + K_3 \cos^2 \theta(z,t)] \frac{\partial^2 \theta(z,t)}{\partial z^2}, \tag{19}$$

where K_1 and K_3 are the splay and bend elastic constants, respectively; γ_1 is the rotational viscosity coefficient, and the dielectric torque is of the form

$$\begin{aligned} M(t) = \varepsilon_0 E(t) \Bigg\{ & (\varepsilon_{f\parallel} - \varepsilon_{f\perp}) \sin \theta(z,t) \cos \theta(z,t) E(t) \\ & + \sin \theta(z,t) \int_{-\infty}^{t} \cos \theta(z,t') \sum_{i=1}^{p_\parallel} \frac{\delta \varepsilon_{i\parallel}}{\tau_{i\parallel}} \\ & \times \exp\left(- \frac{t-t'}{\tau_{i\parallel}} \right) E(t') dt' \\ & - \cos \theta(z,t) \int_{-\infty}^{t} \sin \theta(z,t') \sum_{j=1}^{p_\perp} \frac{\delta \varepsilon_{j\perp}}{\tau_{j\perp}} \\ & \times \exp\left(- \frac{t-t'}{\tau_{j\perp}} \right) E(t') dt' \Bigg\}. \end{aligned} \tag{20}$$

Equations (19) and (20) determine the profile of $\theta(z,t)$—i.e., the temporal and spatial profile of the director field. Since $\hat{\mathbf{n}}$ is simultaneously the optical axis in the uniaxial nematic LC, its behavior can be traced experimentally by measuring the light intensity transmitted through the cell and a pair of crossed linear polarizers. When the x axis is at an angle of 45° to the axes of the two polarizers, Fig. 1, the (normalized) transmitted light intensity

$$I(t) = \sin^2 \frac{\Delta \varphi(t)}{2} \tag{21}$$

is determined by the optical phase shift of the nematic cell [17],

$$\Delta \varphi(t) = \frac{2\pi n_o}{\lambda} \int_0^d [n_e / \sqrt{n_o^2 \sin^2 \theta(z,t) + n_e^2 \cos^2 \theta(z,t)} - 1] dz, \tag{22}$$

where n_o and n_e are the ordinary and extraordinary refractive indices of the LC, respectively; d is the cell gap. Since we are only interested in a short time interval at the beginning of switching where the DME occurs—i.e., in about a few tens of nanoseconds for the case of 5CB and a few tens of microseconds for conventional DFNs—the backflow effect, whose characteristic time is in the range of milliseconds [18,19], can be ignored, which justifies the form of Eq. (19).

Equation (20) clearly demonstrates how the relaxation processes will affect the director dynamics. Depending on the rate with which the electric field is changing, any relaxation process would qualify either as "fast" (if its relaxation time is shorter than τ_U) or as "slow." The "fast" contributes to the "instantaneous" torque represented by the first term in Eq. (20). The "slow" contributes to one of the two "memory" integrals in Eq. (20) associated with either the parallel or perpendicular component. The instantaneous and memory torques corresponding to different relaxation processes have generally different "strengths" determined by $(\varepsilon_{f\parallel} - \varepsilon_{f\perp})$ that might be both positive and negative and by $\delta\varepsilon_{i\eta}$ that is always positive, but enters Eq. (20) with a "+" sign for the parallel component and a "−" sign for the perpendicular component. The balance of all these contributions would define the temporal behavior of $\hat{\mathbf{n}}$, including situations when the sense of director reorientation reverses with time. In the experimental part, we discuss situations that highlight different contributions to Eq. (20).

III. EXPERIMENTAL SETUP

We choose three types of nematic materials (all purchased from E.M. Industries): (A) The classic nematic 5CB in which both $\varepsilon_\parallel$ and $\varepsilon_\perp$ experience dielectric relaxation with characteristic times in the range of 1–100 ns [9,10]. (B) Nematic mixtures of 5CB and MLC2048 in which we observe multiple dielectric relaxations of $\varepsilon_\parallel$. MLC2048 is a conventional DFN; although it is by itself a mixture, it shows a single relaxation time and $f_c = 12$ kHz at room temperature [20]. Multiple relaxations in $\varepsilon_\parallel$ of the 5CB+MLC2048 mixtures at different frequencies originate from the relaxations of different molecular components of the mixture. (C) Nematic mixture of MLC7026-100 and MLC2048, in which $\Delta\varepsilon$ is negative for all frequencies and $\varepsilon_\parallel$ experiences a single relaxation.

The cells were constructed by bonding two glass substrates coated with transparent indium tin oxide (ITO) electrodes. In all experimental cells, on top of ITO, we used alignment layers that allow one to maximize the dielectric

torque acting on $\hat{\mathbf{n}}$, which implies that $\hat{\mathbf{n}}$ and $\mathbf{E}$ make an angle close to 45° [5].

(A) The 5CB cells were constructed with a reduced active area of the electrodes, about 500×500 μm^2 (through photolithography patterning). An additional layer of gold is coated as the electric leads to the ITO areas. The purpose of using a small active area and gold coating is to reduce the *RC* load of the circuit, and thus to reduce the delay of the electric field applied to the cell [4]; the estimated delay from the *RC* load was 0.5 ns. As an alignment layer, we deposited a SiO_x film on top of the gold and the ITO layers. The actual tilt angle θ_b between $\hat{\mathbf{n}}$ and the z axis was determined to be 51.2° by measuring the phase shift with a Soleil Babinet SB-10 (Optics for Research) optical phase compensator. The cell gap was 4.4 μm as determined by the interference method.

(B) The cells with 5CB+MLC2048 mixtures were assembled with an active area of ITO of about 1×1 mm^2. The estimated delay from the *RC* load was 20 ns—i.e., much lower than the shortest relaxation time ~200 ns measured for these mixtures. The alignment layer was a SiO_x film, yielding $\theta_b=50.2°$. The cell gap was 3.5 μm.

(C) The cells with MLC7026-100 and MLC2048 mixtures were assembled with a larger active area of about 25×25 mm^2. The delay from the *RC* load was 0.3 μs, which is lower than the typical relaxation times 2 μs of these mixtures. The alignment layer was a mixture of polyimide PI2555 (DuPont) and polyimide JSR659AL (Japan Synthetic Rubber) in proportion 95–5 wt %, yielding $\theta_b=20.5°$. The cell gap was 12.5 μm.

The cells were placed between two crossed polarizers with the cell's x axis making an angle 45° with the transmission axes of the crossed polarizer and analyzer, Fig. 1. The optical phase compensator SB-10 with a controllable phase delay $\Delta\varphi'$ is inserted between the cell and the analyzer in order to adjust the normalized transmitted light intensity,

$$I(t)=\sin^2\left(\frac{\Delta\varphi(t)+\Delta\varphi'}{2}\right), \tag{23}$$

in such a way that in the absence of an electric field, $I(t)$ is about 1/2 of its maximum possible value. For this setting, the sensitivity of the system to the light intensity change caused by the director reorientation is maximized. We have chosen $\Delta\varphi'$ in such a way that a field-induced (small) reorientation of $\hat{\mathbf{n}}$ *parallel* to $\mathbf{E}$ corresponds to an *increase* of $I(t)$. The intensity of the laser beam (He-Ne laser, 633 nm) that passes through the cell is measured by a TIA-500S-TS photodetector (Terahertz Technologies Inc.) with the response time less than 1 ns. The recorded signal is displayed on a Tektronix TDS 210 digital oscilloscope, which is connected to a computer via IEEE-488 cable for data storage and analysis [IEEE-488 is also commonly known as the general purpose interface bus (GPIB)].

In order to observe the DME in 5CB, the rise time of the voltage, τ_U, should be comparable to or less than the dielectric relaxation time τ_r of 5CB, which is only a few tens of nanoseconds in the nematic phase [10]. We use a pulse generator HV1000 (Direct Energy Inc.) capable of producing any voltage pulse up to 1000 V. The time evolution $U(t)$ of the pulse front for this generator can be approximated by the exponential function $U(t)=U_0[1-\exp(-t/\tau_U)]$, where $\tau_U=6$ ns.

In the nanosecond range, one needs to take particular care of any factors influencing the data, such as the cell area (see above) and the finite speed of signal propagation. For a typical 50-Ω coaxial electric cable, this speed is ~$0.8c$, where c is the speed of light in vacuum; the signal needs roughly 4 ns to propagate by about 1 m. For our experimental setup, Fig. 1, we measured the time difference for signal propagation between two arms connecting the nematic cell and the oscilloscope. One arm is comprised of the laser beam propagation between the cell and the photodetector and the electric signal propagation to the oscilloscope through cable $C1$; the second arm is the electrical connection for the applied voltage through cable $C2$, Fig. 1. We determined the time difference between these two arms to be 16 ns. This time difference was used to synchronize the data coming through the two arms.

To observe the DME in DFNs and in nematics with negative dielectric anisotropy, in which τ_r is much longer than in 5CB, we used the wave-form generator WFG500 (FLC Electronics AB) combined with a KH7602M amplifier (Krohn-Hite Corporation). The voltage increase rate was 476 V/μs.

The experiments were performed at the temperature 23 °C and 30 °C for 5CB (at which the dielectric parameters have been determined for a broad range of frequencies [9,10]). For the rest of materials and mixtures, the experiments were performed at room temperature, close to 23 °C; the frequency dependences of permittivities were measured in the laboratory by using the Schlumberger 1260 impedance/gain-phase analyzer.

IV. RESULTS AND DISCUSSION

A. 5CB: Dielectric relaxations in both $\varepsilon_\parallel$ and $\varepsilon_\perp$

5CB is a material of the so-called "dielectrically positive" type, which means that at low frequencies (up to the MHz region), $\Delta\varepsilon=\varepsilon_\parallel-\varepsilon_\perp>0$. As demonstrated by Gestblom and Wróbel [11] and Belyaev *et al.* [9,21], both $\varepsilon_\parallel$ and $\varepsilon_\perp$ show relaxation with different characteristic times, so that $\Delta\varepsilon$ changes sign from positive to negative and then back to positive as the frequency increases. The $\varepsilon_\parallel$ component shows even two relaxation processes [9]; however, the second process has a relaxation time less than 1 ns and can be neglected in our experiment with $\tau_U\sim10$ ns. We model the dielectric dispersion curves of 5CB using the Debye approach [14]:

$$\varepsilon_\parallel(\omega)=\varepsilon_{h\parallel}+\frac{\varepsilon_{l\parallel}-\varepsilon_{h\parallel}}{1-i\omega\tau_\parallel},\quad \varepsilon_\perp(\omega)=\varepsilon_{h\perp}+\frac{\varepsilon_{l\perp}-\varepsilon_{h\perp}}{1-i\omega\tau_\perp}, \tag{24}$$

where the subscripts l and h refer to the low-frequency and high-frequency values of the permittivities, respectively.

The dielectric properties in LCs are temperature dependent, as studied for 5CB by a number of research groups [9–12,21–27]. We first discuss the dispersion curves, Eqs. (24), for two different temperatures, 30 °C and 23 °C, for which the most literature data are available.

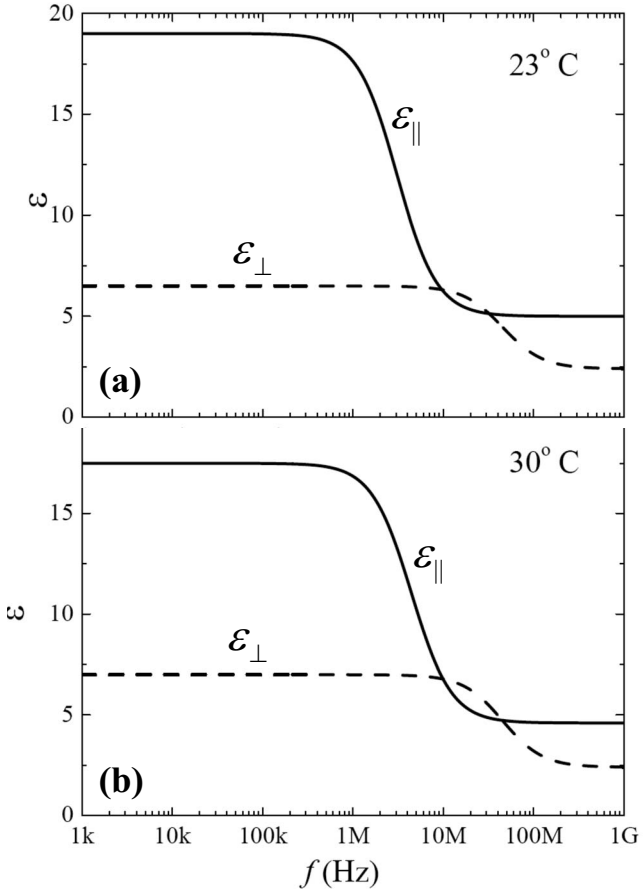

FIG. 2. Dielectric dispersion curves of 5CB based on the Debye model, Eq. (24), where $\varepsilon_{l\parallel}=19.0$, $\varepsilon_{h\parallel}=5.0$, and $\tau_{\parallel}=64$ ns; $\varepsilon_{l\perp}=6.5$, $\varepsilon_{h\perp}=2.4$, and $\tau_{\perp}=3.5$ ns for 23 °C (a) and $\varepsilon_{l\parallel}=17.5$, $\varepsilon_{h\parallel}=4.6$, and $\tau_{\parallel}=36$ ns; $\varepsilon_{l\perp}=7$, $\varepsilon_{h\perp}=2.4$, and $\tau_{\perp}=3.5$ ns for 30 °C (b).

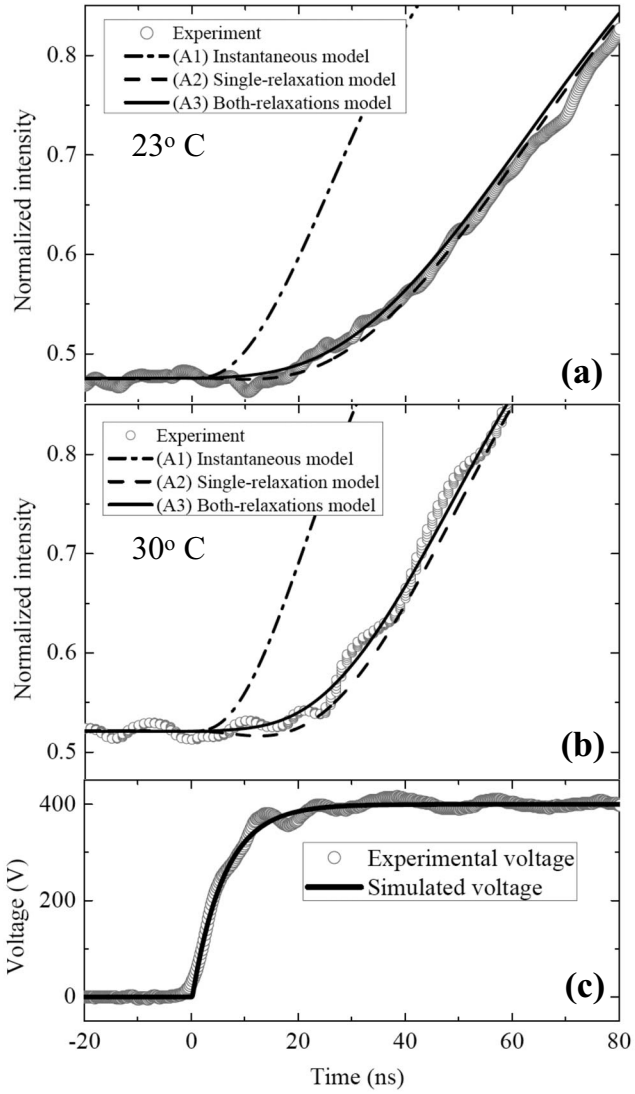

FIG. 3. Normalized light intensity (a), (b) transmitted by the electrically driven 5CB cell and a pair of crossed polarizers as a function of time at 23 °C (a) and 30 °C (b). (c) Applied voltage with simulated time dependence (solid curve). The circles are the experimental data; the curves in (a) and (b) represent simulations with different models as indicated by the labels.

For 30 °C, to fit $\varepsilon_{\parallel}(\omega)$, we used $\varepsilon_{l\parallel}=17.5$ measured by Cummins *et al.* [22] and $\varepsilon_{h\parallel}=4.6$ measured by Belyaev *et al.* [9,21]. We also used $\tau_{\parallel}=36$ ns from the experiment by Kreul *et al.* [10]. For $\varepsilon_{\perp}(\omega)$ at 30 °C, we use $\varepsilon_{l\perp}=7.0$ measured in Ref. [22] and $\varepsilon_{h\perp}=2.4$ and $\tau_{\perp}=3.5$ ns from the experiments in Refs. [9,21].

For 23 °C, to fit $\varepsilon_{\parallel}(\omega)$, we measured $\varepsilon_{l\parallel}=19.0$ in our laboratory [28] and determined $\varepsilon_{h\parallel}=5.0$ from the expression $\delta\varepsilon_{\parallel}=\varepsilon_{l\parallel}-\varepsilon_{h\parallel}=2\varepsilon''_{\max}$, where $\varepsilon''_{\max}\approx 7$ is the maximum of the imaginary part of the parallel dielectric permittivity measured at 23 °C in Ref. [23]. We used $\tau_{\parallel}=64$ ns from the experiments by Kreul *et al.* [10], which were also performed at 23 °C. For $\varepsilon_{\perp}(\omega)$, we measured $\varepsilon_{l\perp}=6.5$ and used $\varepsilon_{h\perp}=2.4$ and $\tau_{\perp}=3.5$ ns from the experiments in Refs. [9,21]. The last two values have been measured at 30 °C; however, we do not expect significant temperature changes for $\varepsilon_{h\perp}$ and $\tau_{\perp}$ because of the barrier-free character of the corresponding relaxation process.

With the parameters above, one can reconstruct the frequency dependences of dielectric permittivities for 5CB, Eq. (24), Fig. 2. These data closely resemble the experimental findings in Refs. [9–12,21–23]. Namely, at $f>9$ MHz for 23 °C and 10 MHz for 30 °C, 5CB behaves as a dielectrically *negative* material with $\Delta\varepsilon<0$, while at even higher frequencies, $f>32$ MHz for 23 °C and 45 MHz for 30 °C, it returns to $\Delta\varepsilon>0$.

With the dielectric dispersion of 5CB modeled in Fig. 2, we now proceed to a study of the DME by exploring the director dynamics at the very beginning of a sharp voltage pulse, Fig. 3. The most interesting feature is that within the first 15 ns of the voltage pulse, the optical signal changes very little, despite a sharp increase of the field. A similar "delay" phenomenon has been observed by Takanashi *et al.* [4] for a similar 5CB cell driven by similar sharp pulses. The experiments in both Takanashi *et al.* and our case were designed to reduce the delays in the optical response associated with finite rise time of the equipment used. Namely, in our case all the relevant rise time (in the *RC* circuit, photodetector, and oscilloscope) were each about 1 ns or less; see Sec.

III. Therefore, the "delay" in optical response cannot be attributed to the finite rise time of the experimental setup. Clark and co-authors [4,29] came to the same conclusion and suggested that the delay might be caused by the dielectric relaxation. Below we demonstrate that our model above does provide both a qualitative and quantitative explanation of the delay as the result of dielectric relaxation.

To fit the experimental data in Fig. 3, we used three theoretical models of dielectric response: namely, (i) the standard instantaneous approach, (ii) the single-relaxation model [6], and (iii) the present model in which both $\varepsilon_{\|}$ and $\varepsilon_{\perp}$ relaxations are taken into consideration. The dielectric torque, Eq. (20), assumes different forms in these three models. Namely, $\varepsilon_{f\eta}$ in Eq. (20) should be taken as $\varepsilon_{h\eta}$ and $\delta\varepsilon_{\eta}=\varepsilon_{l\eta}-\varepsilon_{h\eta}$ if one takes into account the relaxation of a corresponding permittivity component and as $\varepsilon_{l\eta}$ if one assumes no relaxation (in which case, obviously, $\delta\varepsilon_{\eta}=0$). Therefore, the dielectric torque has the following forms in the three models.

(A1) In the standard instantaneous approach, in which we neglect all the dielectric relaxation processes,

$$M_{\mathrm{A1}}(t)=\varepsilon_0(\varepsilon_{f\|}-\varepsilon_{f\perp})\sin\theta(z,t)\cos\theta(z,t)E^2(t), \quad (25)$$

where $\varepsilon_{f\|}=19.0$ and $\varepsilon_{f\perp}=6.5$ for 23 °C and $\varepsilon_{f\|}=17.5$ and $\varepsilon_{f\perp}=7.0$ for 30 °C (according to the data for 5CB in Fig. 2).

(A2) In the single-relaxation model [6], where only the dielectric relaxation of $\varepsilon_{\|}$ is considered:

$$M_{\mathrm{A2}}(t)=\varepsilon_0 E(t)\sin\theta(z,t)\left\{(\varepsilon_{f\|}-\varepsilon_{f\perp})\cos\theta(z,t)E(t)+\int_{-\infty}^{t}\cos\theta(z,t')\frac{\delta\varepsilon_{\|}}{\tau_{\|}}\exp\left(-\frac{t-t'}{\tau_{\|}}\right)E(t')dt'\right\}, \quad (26)$$

where $\delta\varepsilon_{\|}=14.0$, $\varepsilon_{f\|}=5.0$, and $\tau_{\|}=64$ ns; $\varepsilon_{f\perp}=6.5$ for 23 °C; $\delta\varepsilon_{\|}=12.9$, $\varepsilon_{f\|}=4.6$, and $\tau_{\|}=36$ ns; $\varepsilon_{f\perp}=7.0$ for 30 °C (according to Fig. 2).

(A3) In the present model in which both $\varepsilon_{\|}$ and $\varepsilon_{\perp}$ relaxations are taken into consideration:

$$M_{\mathrm{A3}}(t)=\varepsilon_0 E(t)\left\{(\varepsilon_{f\|}-\varepsilon_{f\perp})\sin\theta(z,t)\cos\theta(z,t)E(t)+\sin\theta(z,t)\int_{-\infty}^{t}\cos\theta(z,t')\frac{\delta\varepsilon_{\|}}{\tau_{\|}}\times\exp\left(-\frac{t-t'}{\tau_{\|}}\right)E(t')dt'-\cos\theta(z,t)\int_{-\infty}^{t}\sin\theta(z,t')\frac{\delta\varepsilon_{\perp}}{\tau_{\perp}}\exp\left(-\frac{t-t'}{\tau_{\perp}}\right)E(t')dt'\right\}. \quad (27)$$

where $\delta\varepsilon_{\|}=14.0$, $\varepsilon_{f\|}=5.0$, and $\tau_{\|}=64$ ns; $\delta\varepsilon_{\perp}=4.1$, $\varepsilon_{f\perp}=2.4$, and $\tau_{\perp}=3.5$ ns for 23 °C; $\delta\varepsilon_{\|}=12.9$, $\varepsilon_{f\|}=4.6$, and $\tau_{\|}=36$ ns; $\delta\varepsilon_{\perp}=4.6$, $\varepsilon_{f\perp}=2.4$, and $\tau_{\perp}=3.5$ ns for 30 °C, as in Fig. 2.

With the known values of the dielectric torque, Eq. (25)–(27), one can simulate the dynamics of $\hat{\mathbf{n}}$ using Eq. (19) and then simulate the corresponding changes in the intensity of light transmitted through the cell and polarizers using Eqs. (22) and (23). In the Erickson-Leslie equation (19), one can neglect the elastic term. The reason is that for high voltages, $\hat{\mathbf{n}}$ reorients practically uniformly in the bulk of cell, with elastic distortions taking place only within a very thin layer near the substrates. As the voltage used 400 V, is about 400 times larger than the Frederiks threshold for 5CB, the thickness of the subsurface layer where $\hat{\mathbf{n}}$ experiences distortions is only $\xi\sim d\sqrt{\Delta\theta}/400\sim 1$ nm; here, $\Delta\theta\sim 0.01$ rad (or less) is the angle of $\hat{\mathbf{n}}$ reorientation during the "delay" interval (the estimate follows from the fact that the phase retardation does not change much during this period). Therefore, the elastic contribution in Eq. (19) to the transmitted light intensity changes is negligibly small as compared to the dielectric term, as the ratio $\xi/d<10^{-3}$ is very small.

The electric pulse was simulated as $U(t)=U_0[1-\exp(-t/\tau_U)]$, where $\tau_U=6$ ns, Fig. 3. In Eq. (19), we used values of rotational viscosity $\gamma_1=0.1$ kg m^{-1} s^{-1} at 23 °C and $\gamma_1=0.059$ kg m^{-1} s^{-1} at 30 °C, as measured by Wu and Wu [30]. Finally, in the simulations of light transmission, Eqs. (22) and (23), we used $n_o=1.52$ and $n_e=1.70$ for both temperatures, as measured in our laboratory at 633 nm.

The simulated light transmittance in Fig. 3 clearly demonstrates that the "delay" effect is well described by the dielectric relaxation model. The standard instantaneous approach (A1) predicts no delay (except for the first few nanoseconds when the exponentially growing voltage still remains relatively low). The models (A2) and (A3) of dielectric relaxation both show that the optical response is delayed with respect to the front of electric pulse. The delay is caused by the "wrong" sense of director reorientation at the beginning of the electric pulse. The sharp front of the pulse is perceived by the LC as a high-frequency excitation, at which the dielectric anisotropy $\Delta\varepsilon$ is different from the low-frequency values. In particular, the model (A2), which accounts only for the relaxation of $\varepsilon_{\|}$, predicts an initial decrease in $I(t)$, as at the high frequency, $\Delta\varepsilon=\varepsilon_{h\|}-\varepsilon_{l\perp}<0$ and $\hat{\mathbf{n}}$ reorients away from the field. After some time, $\hat{\mathbf{n}}$ begins to reorient toward $\mathbf{E}$, as $\Delta\varepsilon>0$ at low f. Although the model (A2) explains the apparent delay (as the result of an initially "wrong" direction of reorientation), it slightly overestimates the effect, as it considers $\Delta\varepsilon$ always negative at high f. The model (A3), which accounts for relaxations of both components, is a bit more accurate, as it is only in the limited frequency region, between the relaxation frequencies for $\varepsilon_{\|}$ and $\varepsilon_{\perp}$, that $\Delta\varepsilon<0$. At higher f, above the relaxation frequency of $\varepsilon_{\perp}$, $\Delta\varepsilon$ is positive. As a result, in response to the sharp voltage pulse, $\hat{\mathbf{n}}$ reorients first *toward* $\mathbf{E}$, then *away* from $\mathbf{E}$, and then *toward* $\mathbf{E}$ again. It appears that the model (A3) is the best suited to fit the experiment, although the noise of experimental data does not allow one to see clearly an increase in the $I(t)$ curve caused by the initial rotation of $\hat{\mathbf{n}}$ toward $\mathbf{E}$.

Note that the literature data on $\tau_{\|}$ show some scattering. For example, Belyaev *et al.* [9] reported $\tau_{\|}\approx 25$ ns for 30 °C instead of 36 ns in [10] used in our simulations. With $\tau_{\|}$

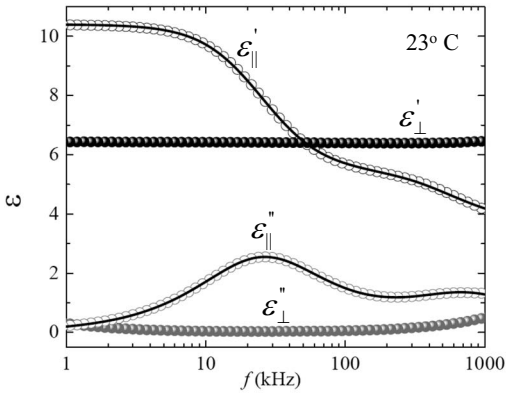

FIG. 4. Experimental data on dielectric dispersion curves of the mixture with 7.0 wt. % 5CB and 93.0 wt. % MLC2048 for the real components ($\varepsilon'_{\parallel}$, $\varepsilon'_{\perp}$) and the imaginary components ($\varepsilon''_{\parallel}$, $\varepsilon''_{\perp}$) at room temperature 23 °C. The solid curves are fitted with Eq. (28), where $\varepsilon_{l\parallel}=10.4$, $\varepsilon_{m\parallel}=5.3$, $\varepsilon_{h\parallel}=3.5$, $\varepsilon_{\perp}=6.4$, $\tau_1=6.0$ μs, and $\tau_2=0.23$ μs.

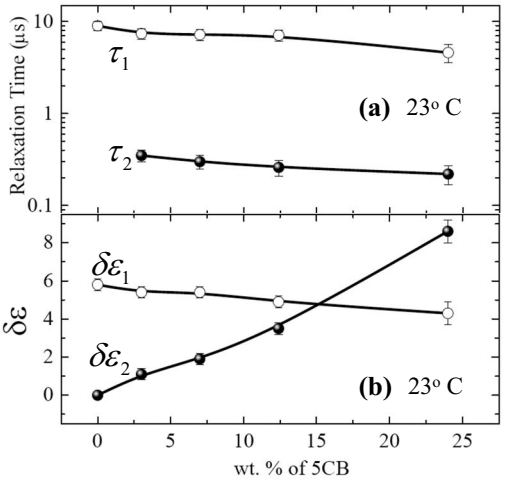

FIG. 5. The first and second dielectric relaxation times (a) and dielectric strength (b) of the parallel component $\varepsilon_{\parallel}$ of 5CB +MLC2048 mixtures versus the weight concentration of 5CB at 23 °C.

≈ 25 ns, the simulations still produce a delayed response, but the agreement with the experiment is not good and cannot be improved by varying other parameters such as rotational viscosity. We thus consider the values used in the dielectric dispersion model, Eq. (24) and Fig. 2, as the best choice for the characterization of 5CB.

B. 5CB-MLC2048 mixtures: Multiple relaxations in $\varepsilon_{\parallel}$

In this section, we explore the director dynamics in materials with multiple relaxations in $\varepsilon_{\parallel}$ and little or no relaxation in $\varepsilon_{\perp}$. The experimental system is a mixture of 5CB and MLC2048 that shows a Debye type of dielectric relaxation, as evidenced by fitting the experimental data with the expression

$$\varepsilon_{\parallel}(\omega) = \varepsilon_{h\parallel} + \frac{\varepsilon_{l\parallel} - \varepsilon_{m\parallel}}{1 - i\omega\tau_1} + \frac{\varepsilon_{m\parallel} - \varepsilon_{h\parallel}}{1 - i\omega\tau_2}. \quad (28)$$

Figure 4 illustrates an example of the mixture comprised of 7.0 wt % 5CB and 93.0 wt % MLC2048, in which the dispersion curves are well fitted by Eq. (28) with $\varepsilon_{l\parallel}=10.4$, $\varepsilon_{m\parallel}=5.3$, $\varepsilon_{h\parallel}=3.5$, $\varepsilon_{\perp}=6.4$, $\tau_1=6.0$ μs and $\tau_2=0.23$ μs. The fitting parameters vary with the composition of the mixtures. In Fig. 5, we present the concentration dependencies for relaxation times τ_1 and τ_2 and for the dielectric relaxation "strength" $\delta\varepsilon_1=\varepsilon_{l\parallel}-\varepsilon_{m\parallel}$ and $\delta\varepsilon_2=\varepsilon_{m\parallel}-\varepsilon_{h\parallel}$.

The results of the DME experiment for the mixture with 7.0 wt % 5CB and 93.0 wt % MLC2048 driven by a sharply increasing dc pulse are shown in Fig. 6. The voltage increases from 0 V to 200 V practically linearly, over 0.42 μs. The experimental optical response corresponds to the director reorientation initially *perpendicular* to **E** over the first ~ 2 μs (i.e., toward the planar state in the geometry of experiment), followed by its reorientation *towards* **E** at the later times. Physically, the sharp front of pulse is perceived by the mixture as a high-frequency excitation for which the dielectric anisotropy is negative. To fit the data, we again used three models, in which $\varepsilon_{\perp}=6.4$ remains constant.

(B1) The standard instantaneous approach, in which all the dielectric relaxation processes are neglected,

$$M_{\mathrm{B1}}(t) = \varepsilon_0(\varepsilon_{f\parallel} - \varepsilon_{\perp})\sin\theta(z,t)\cos\theta(z,t)E^2(t), \quad (29)$$

where $\varepsilon_{f\parallel}=10.4$ (according to Fig. 4).

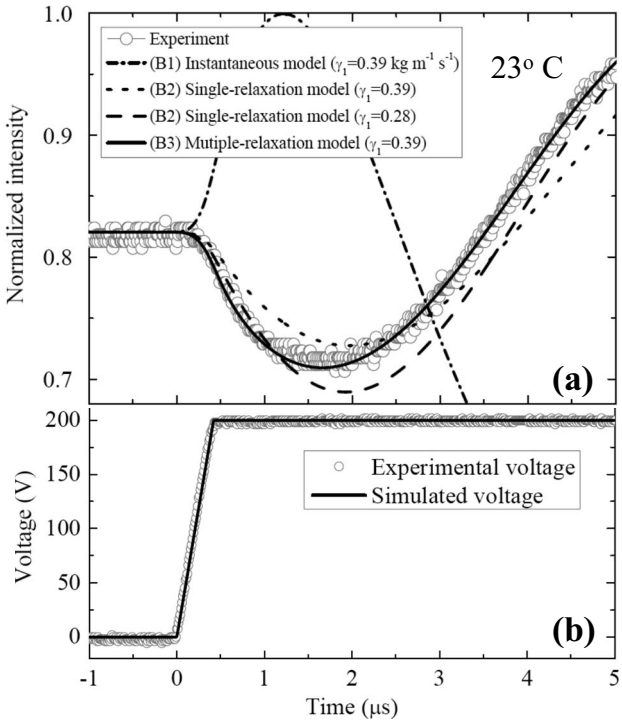

FIG. 6. Normalized transmitted light intensity versus time (a) for 7.0 wt. % 5CB+93.0 wt. % MLC2048 mixture driven by fast-changing rectangular pulse (b). The circles are the experimental data; the curves represent simulations with different models as indicated by the labels.

(B2) The single-relaxation model [6], where only one dielectric relaxation of $\varepsilon_{\|}$ is considered:

$$M_{\mathrm{B2}}(t) = \varepsilon_0 E(t)\sin\theta(z,t)\left\{(\varepsilon_{f\|} - \varepsilon_{\perp})\cos\theta(z,t)E(t) + \int_{-\infty}^{t} \cos\theta(z,t')\frac{\delta\varepsilon_1}{\tau_1}\exp\left(-\frac{t-t'}{\tau_1}\right)E(t')dt'\right\}, \tag{30}$$

with $\delta\varepsilon_1 = 5.1$, $\varepsilon_{f\|} = 5.3$, and $\tau_1 = 6.0$ μs, Fig. 4.

(B3) The present model with both relaxations of $\varepsilon_{\|}$ taken into consideration:

$$M_{\mathrm{B3}}(t) = \varepsilon_0 E(t)\sin\theta(z,t)\left\{(\varepsilon_{f\|} - \varepsilon_{\perp})\cos\theta(z,t)E(t) + \int_{-\infty}^{t} \cos\theta(z,t')\left[\frac{\delta\varepsilon_1}{\tau_1} \times \exp\left(-\frac{t-t'}{\tau_1}\right) + \frac{\delta\varepsilon_2}{\tau_2}\exp\left(-\frac{t-t'}{\tau_2}\right)\right]E(t')dt'\right\}, \tag{31}$$

with $\delta\varepsilon_1 = 5.1$, $\delta\varepsilon_2 = 1.9$, $\tau_1 = 6.0$ μs, $\tau_2 = 0.23$ μs, and $\varepsilon_{f\|} = 3.5$, as in Fig. 4.

In computer simulations of the optical response, we used $n_o = 1.501$ and $n_e = 1.718$ in Eq. (22), measured in the laboratory, and $\gamma_1 = 0.39$ kg m^{-1} s^{-1} in Eq. (19), as obtained by fitting the experimental data in Fig. 6.

Comparison of the experimental and simulated data in Fig. 6 demonstrates that the two-relaxation model (B3) fits the experiment very well. The instantaneous model (B1) predicts a wrong direction of reorientation while the single-relaxation model (B2) does predict the initial reorientation of $\hat{\mathbf{n}}$ perpendicular to $\mathbf{E}$ but does not agree with the experimental data in details. One can attempt to modify the parameters of model (B2) to better fit the data. For example, we change the rotational viscosity γ_1 in an attempt to better fit the experiment, dashed curve in Fig. 6, yet it is not as good as the fitting by the model (B3).

C. MLC7026-100-MLC2048 mixture: $\Delta\varepsilon < 0$ with a single relaxation in $\varepsilon_{\|}$

So far, we considered nematic LCs in which the static $\Delta\varepsilon$ is positive and the high-frequency $\Delta\varepsilon$ is smaller or even negative. Because of this, the DME slows down the director reorientation driven by sharp voltage pulses, as the front of pulse is perceived as a high-frequency excitation. In these materials, a faster response time can thus be obtained by taking τ_U *longer* rather than shorter [31]. However, in the case of nematic LCs in which the static $\Delta\varepsilon$ is negative, the DME might lead to faster director reorientation if the high-frequency $\Delta\varepsilon$ is larger (in absolute value) than its low-frequency counterpart. Since negative-anisotropy materials are of prime importance in the flat-panel display industry, forming the basis of the so-called "patterned vertical alignment" technology [32,33], we conclude this work with a short illustration of the DME in these materials.

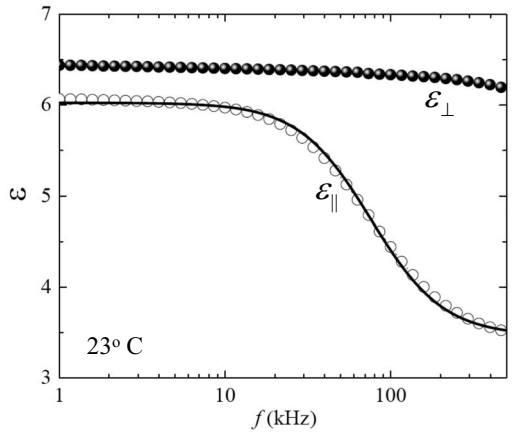

FIG. 7. Dielectric dispersion curves for the real components ($\varepsilon_{\|}$, $\varepsilon_{\perp}$) of the mixture 53.7 wt. % MLC7026-100+46.3 wt. % MLC2048 at 23 °C. The solid curve is fitted with Eq. (24) where $\varepsilon_{h\|} = 3.5$, $\varepsilon_{l\|} = 6.0$, and $\tau_{\|} = 2.1$ μs.

We studied a dielectrically negative mixture obtained by mixing MLC7026-100 and DFN MLC2048 in weight proportion 53.7%: 46.3%. The mixture shows a relaxation in $\varepsilon_{\|}$, Fig. 7. The data can be fitted with the Debye model, Eq. (24), using $\varepsilon_{l\|} = 6.0$, $\varepsilon_{h\|} = 3.5$, and $\tau_{\|} = 2.1$ μs. The relaxation time of the perpendicular component is smaller than 40 ns, and thus we consider this component as a constant, $\varepsilon_{\perp} = 6.4$.

In Fig. 8, we illustrate the effect of a rectangular pulse with a rise time of 0.5 μs. The experimental change in transmitted light intensity corresponds to the director reorientation away from $\mathbf{E}$ for the whole driving interval. Physically, the sharp rising front of the pulse is perceived as a high-frequency excitation at which $\Delta\varepsilon$ remains negative but acquires an even larger absolute value as compared to that at the low frequencies. To fit the experiment, we used two models.

(C1) The standard instantaneous approach, in which all the dielectric relaxation processes are neglected,

$$M_{\mathrm{C1}}(t) = \varepsilon_0(\varepsilon_{f\|} - \varepsilon_{\perp})\sin\theta(z,t)\cos\theta(z,t)E^2(t), \tag{32}$$

where $\varepsilon_{f\|} = 6.0$, $\varepsilon_{\perp} = 6.4$, according to Fig. 7.

(C2) The DME model in which the relaxation of $\varepsilon_{\|}$ is taken into consideration:

$$M_{\mathrm{C2}}(t) = \varepsilon_0 E(t)\sin\theta(z,t)\left\{(\varepsilon_{f\|} - \varepsilon_{\perp})\cos\theta(z,t)E(t) + \int_{-\infty}^{t} \cos\theta(z,t')\frac{\delta\varepsilon}{\tau}\exp\left(-\frac{t-t'}{\tau}\right)E(t')dt'\right\}, \tag{33}$$

where $\delta\varepsilon = 2.5$, $\varepsilon_{f\|} = 3.5$, $\varepsilon_{\perp} = 6.4$, and $\tau = 2.1$ μs, according to Fig. 7.

In simulations of the optical response, we used $n_o = 1.49$ and $n_e = 1.65$ (measured in the laboratory) and $\gamma_1 = 0.15$ kg m^{-1} s^{-1} obtained by fitting the experimental data below.

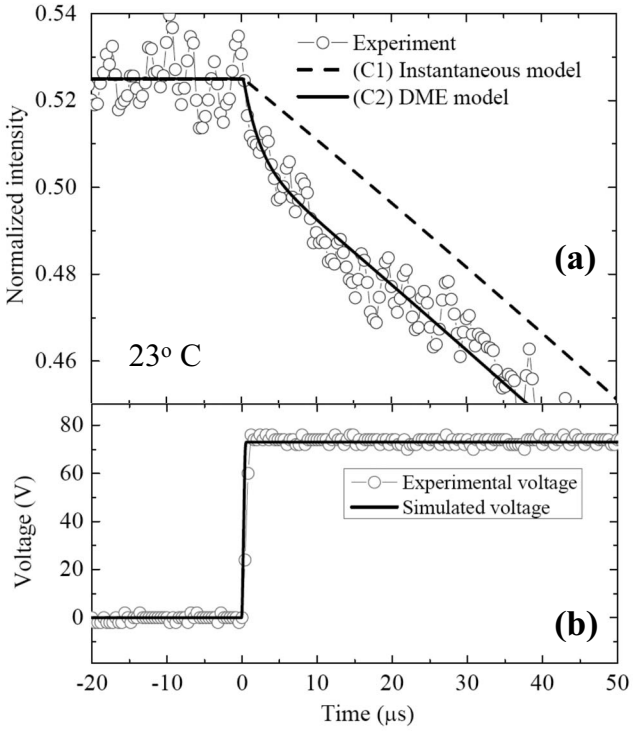

FIG. 8. Normalized transmitted light intensity (a) and voltage (b) versus time for the mixture 53.7 wt. % MLC7026-100 +46.3 wt. % MLC2048 driven by a fast-changing rectangular pulse. The circles are the experimental data; the curves represent simulations with different models as indicated by the labels.

Figure 8 demonstrates that the DME model (C2) explains the experimental data well, while the instantaneous model (C1) predicts a slower director reorientation as compared to the experiment. The accelerated director reorientation seen in the experiment is a result of the DME as the absolute value of $\Delta\varepsilon$ increases at higher frequencies and the sharp front of the pulse is perceived by the mixture as such a high-frequency excitation. In what follows, we present other demonstrations of how the DME speeds up the switching of the nematic with $\Delta\varepsilon < 0$.

(a) Sinusoidal versus rectangular modulation of pulses. The cell is driven by ac pulses at 10 kHz, but in the first experiment the voltage is modulated by a sinusoidal curve and in the second experiment it is modulated by a rectangular profile. The rms value of the voltage was the same in both cases (40 V_{rms}). The rectangular profile yields more efficient reorientation, Fig. 9, as the sharp edges of the pulses lead to a larger $|\Delta\varepsilon|$. In contrast, the sinusoidal modulation in Fig. 9 tests only the low-frequency value of $|\Delta\varepsilon|$, which is only $|-0.5|$ at 10 kHz, smaller than $|-2.6|$ at higher frequencies; see Fig. 7.

(b) Optimizing the driving pulse by increasing the number of sharp fronts. We used two different pulses. One was a single 150-μs duration dc pulse of constant polarity, and the other was a signal of the same amplitude and of the same total duration, but with the polarity changed once, effectively corresponding to a higher frequency. From the point of view of a conventional instantaneous model, the two driving

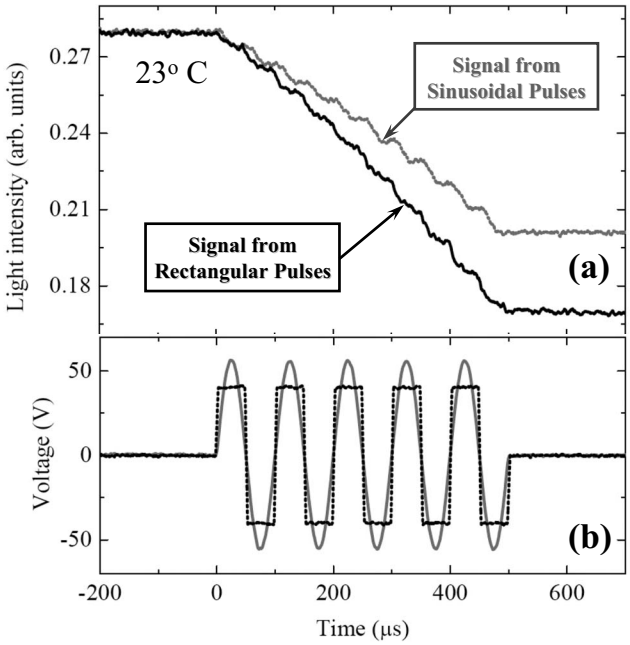

FIG. 9. Transmitted light intensity versus time (a) for the cell filled with the mixture 53.7 wt. % MLC7026-100+46.3 wt. % MLC2048, driven by ac pulses at the same frequency 10 kHz and the same amplitude 40 V_{rms} but of different shapes, a rectangular and sinusoidal one (b).

schemes are equivalent; therefore, there should be no difference in the response time. The experiment, Fig. 10, shows that in fact the second pulse yields a faster reorientation. The

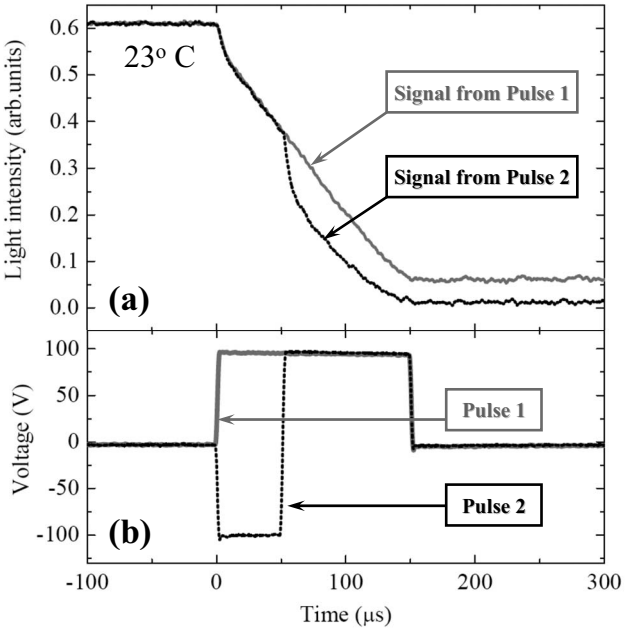

FIG. 10. Transmitted light intensity versus time (a) for the cell filled with the mixture 53.7 wt. % MLC7026-100+46.3 wt. % MLC2048, driven by a dc pulse 1 of duration of 150 μs and amplitude 100 V and by a pulse 2 with a total duration 150 μs and amplitude ±100 V, with polarity changed once (b).

additional sharp front in the second pulse tests the high-frequency values of $|\Delta\varepsilon|$ which are larger than $|\Delta\varepsilon|$ at low frequencies. Note that the fast switching achieved in the industrial cells with patterned vertical alignment (PVA) by using short rectangular pulses of high amplitude might be the result of not only the large amplitude of these "overshooting" signals, but also of their short τ_U [32]. It would be certainly of interest to explore further the optimization of voltage pulses used in PVA mode by incorporating the DME into consideration.

We conclude the discussion with a note that the observed director dynamics in all systems (A), (B), and (C) cannot be attributed to dielectric heating. The latter decreases the scalar order parameter and thus decreases the birefringence $n_e - n_o$. Therefore, the light intensity changes that might have been caused by heating would be of an opposite sign as compared to the observed DME-triggered changes. In addition, the characteristic rates of dielectric heating are too low ($<0.1\ ^\circ\mathrm{C/ms}$) [34] to influence the experimental data reported above in the nanosecond and microsecond range.

V. CONCLUSION

We presented a general model to describe the switching dynamics of uniaxial nematic LCs subject to a changing electric field. We demonstrate that when the characteristic time of voltage change is of order or smaller than the dielectric relaxation time, the director dynamics cannot be explained by conventional dielectric response theory, in which the electric displacement is assumed to be an instantaneous function of the applied field. In the proposed model, we take into consideration that both parallel and perpendicular components of the dielectric permittivity tensor might experience relaxation and that there might be several relaxation processes. The dielectric torque density is determined by the entire frequency spectrum of the dielectric tensor $\varepsilon(\omega)$ rather than by a particular value of the dielectric anisotropy $\Delta\varepsilon$ at any given frequency. In addition, the model takes into account that $\hat{\mathbf{n}}$ changes during the switching process.

The essence of the model is represented by Eq. (20), which expresses the dielectric torque on the director. Depending on the typical time τ_U with which the electric field is changing, any relaxation process would qualify either as "fast" (if its relaxation time is shorter than τ_U) or as "slow." The fast relaxations contribute to the "instantaneous" torque, the first term in Eq. (20). The slow relaxations contribute to one of the two "memory" integrals of Eq. (20), associated with either the parallel or perpendicular component. The balance of "instantaneous" and "memory" contributions defines the temporal behavior of the director, which in some cases is totally opposite to an intuitive picture presented by the standard model.

We used a number of different materials to verify and illustrate the applicability of the proposed model. As an example of the potentially "fastest" (with the highest relaxation frequencies) material with molecules carrying permanent dipoles, we used 5CB. We demonstrate that when the applied voltage changes on the scale of nanoseconds, the dielectric response of 5CB cannot be described by the standard model, but can be described by our model in which the dielectric torque is determined by the two spectral dependences $\varepsilon_\parallel(\omega)$ and $\varepsilon_\perp(\omega)$. A peculiar feature of this dependence on the entire spectra of $\varepsilon_\parallel(\omega)$ and $\varepsilon_\perp(\omega)$ is that the director might experience a "wrong" direction of reorientation, away from the field direction rather than towards it, within the first ~ 10 ns of the applied pulse. The reason is that the sharp front is perceived by the material as the high-frequency excitation at which $\Delta\varepsilon$ might have a value different from the static value and even be of the opposite sign.

In the second experimental system, a 5CB+MLC2048 mixture, we tested multiple relaxations in $\varepsilon_\parallel(\omega)$. Here the "wrong" sense of director reorientation at the beginning of the driving pulse is especially clear as the relaxation time of the mixture is relatively large, 6.0 μs, as compared to the rise time of the voltage we were able to produce in the laboratory. Finally, we presented the third situation, in which $\Delta\varepsilon$ is negative at low frequencies and becomes larger in the absolute value at high frequencies. Here the DME works to speed the switching up rather than to slow it down as in dielectrically positive materials such as 5CB.

The model developed in this work should be of interest in the development of fast-switching LC devices, in which the dielectric relaxation time is comparable to the voltage increase time. In the nematic materials with significant dipole moments, the slowest dielectric relaxation usually corresponds to the flip-flop of the longitudinal dipoles. As a result, in dielectrically positive materials, the DME usually slows down the director response if the applied voltage changes too quickly; therefore, to achieve a faster response, one might need to reduce the rate of voltage changes [31]. In contrast, in negative materials, the DME speeds the response up when the voltage changes quickly.

Obviously, the DME should be also relevant to the electro-optic switching of other materials, such as smectics and biaxial nematics. The latter might represent an especially interesting subject for further studies, as the biaxial nematics offers a possibility of fast switching when the major director remains fixed and the minor director reorients around the major one.

ACKNOWLEDGMENTS

The work was supported by DOE Grant No. DE-FG02-06ER 46331. The authors thank N. Clark and A. Golovin for useful discussions and Liou Qiu for helping with the gold coatings and measurements.

[1] P. G. de Gennes and J. Prost, *The Physics of Liquid Crystals* (Oxford University Press, New York, 1997).
[2] S. T. Wu and D.-K. Yang, *Fundamentals of Liquid Crystal Devices* (Wiley, New York, 2006).
[3] L. M. Blinov and V. G. Chigrinov, *Electrooptic Effects in Liquid Crystal Materials* (Springer-Verlag, New York, 1994).
[4] H. Takanashi, J. E. Maclennan, and N. A. Clark, Jpn. J. Appl. Phys., Part 1 **37**, 2587 (1998).
[5] A. B. Golovin, S. V. Shiyanovskii, and O. D. Lavrentovich, Appl. Phys. Lett. **83**, 3864 (2003).
[6] Y. Yin, S. V. Shiyanovskii, A. B. Golovin, and O. D. Lavrentovich, Phys. Rev. Lett. **95**, 087801 (2005).
[7] N. J. Mottram and C. V. Brown, Phys. Rev. E **74**, 031703 (2006).
[8] W. Haase and S. Wróbel, *Relaxation Phenomena: Liquid Crystals, Magnetic Systems, Polymers, High-Tc Superconductors, Metallic Glasses* (Springer, New York, 2003).
[9] B. A. Belyaev, N. A. Drokin, V. F. Shabanov, and V. A. Baranova, Phys. Solid State **46**, 554 (2004).
[10] H.-G. Kreul, S. Urban, and A. Würflinger, Phys. Rev. A **45**, 8624 (1992).
[11] B. O. Gestblom and S. Wróbel, Liq. Cryst. **18**, 31 (1995).
[12] T. K. Bose, B. Campbell, S. Yagihara, and J. Thoen, Phys. Rev. A **36**, 5767 (1987).
[13] J. D. Jackson, *Classical Electrodynamics* (Wiley, New York, 1962).
[14] P. Debye, *Polar Molecules* (Dover, New York, 1929).
[15] J. L. Erickson, Trans. Soc. Rheol. **5**, 23 (1961).
[16] F. M. Lesile, Arch. Ration. Mech. Anal. **28**, 265 (1968).
[17] M. Kleman and O. D. Lavrentovich, *Soft Matter Physics: An Introduction* (Springer-Verlag, New York, 2003).
[18] D. W. Berreman, J. Appl. Phys. **46**, 3746 (1975).
[19] N. J. Smith, M. D. Tillin, and J. R. Sambles, Phys. Rev. Lett. **88**, 088301 (2002).
[20] Y. Yin, M. Gu, A. B. Golovin, S. V. Shiyanovskii, and O. D. Lavrentovich, Mol. Cryst. Liq. Cryst. **421**, 133 (2004).
[21] B. A. Belyaev, N. A. Drokin, V. F. Shabanov, and V. N. Shepov, Mol. Cryst. Liq. Cryst. Sci. Technol., Sect. A **366**, 305 (2001).
[22] P. G. Cummins, D. A. Dunmur, and D. A. Laidler, Mol. Cryst. Liq. Cryst. **30**, 109 (1975).
[23] B. R. Ratna and R. Shashidhar, Mol. Cryst. Liq. Cryst. **42**, 185 (1977).
[24] F. M. Aliev and N. M. Breganov, Zh. Eksp. Teor. Fiz. **95**, 122 (1989).
[25] S. A. Rozanski, R. Stannarius, H. Groothues, and F. Kremer, Liq. Cryst. **20**, 59 (1996).
[26] S. A. Rozanski, G. P. Sinha, and J. Thoen, Liq. Cryst. **33**, 833 (2006).
[27] F. M. Aliev, M. R. Bengoechea, C. Y. Gao, H. D. Cochran, and S. Dai, J. Non-Cryst. Solids **351**, 2690 (2005).
[28] Yu. A. Nastishin, R. D. Polak, S. V. Shiyanovskii, V. H. Bodnar, and O. D. Lavrentovich, J. Appl. Phys. **86**, 4199 (1999).
[29] Z. Zou, H. Takanashi, G. M. Danner, J. MacLennan, and N. A. Clark, Bull. Am. Phys. Soc. **41**, A17.01 (1996).
[30] S. T. Wu and C. S. Wu, Phys. Rev. A **42**, 2219 (1990).
[31] M. Gu, Y. Yin, S. V. Shiyanovskii, and O. D. Lavrentovich (unpublished).
[32] J. K. Song, K. E. Lee, H. S. Chang, S. M. Hong, M. B. Jun, B. Y. Park, S. S. Seomun, K. H. Kim, and S. S. Kim, SID Int. Symp. Digest Tech. Papers **48**, 1344 (2004).
[33] M. Gu, I. I. Smalykuh, and O. D. Lavrentovich, Appl. Phys. Lett. **88**, 061110 (2006).
[34] Y. Yin, S. V. Shiyanovskii, and O. D. Lavrentovich, J. Appl. Phys. **100**, 024906 (2006).